HHS Public Access

Author manuscript

J Pathol. Author manuscript; available in PMC 2020 October 01.

Published in final edited form as:

J Pathol. 2019 October ; 249(2): 215–226. doi:10.1002/path.5309.

Mitochondrial dysfunction and role of harakiri in the pathogenesis of myositis.

Jessica F Boehler[1,2], **Adam Horn**[1,2], **James Novak**[1,3], **Ning Li**[4], **Svetlana Ghimbovschi**[1], **Ingrid E Lundberg**[5], **Helene Alexanderson**[6], **Li Alemo Munters**[7], **Jyoti K Jaiswal**[1,3,*], **Kanneboyina Nagaraju**[1,4,*]

[1]Center for Genetic Medicine Research, Children's National Health System, 111 Michigan Avenue, NW Washington, DC 20010.

[2]George Washington University, Institute for Biomedical Sciences, Washington, DC.

[3]Department of Genomics and Precision Medicine, George Washington University School of Medicine, Washington, DC.

[4]Department of Pharmaceutical Sciences School of Pharmacy and Pharmaceutical Sciences, Binghamton University, Binghamton, NY.

[5]Division of Rheumatology, Department of Medicine, Solna, Karolinska Institutet, Rheumatology, Karolinska Universitetssjukhuset, Stockholm, Sweden.

[6]Function Area Occupational Therapy and Physical Therapy, Karolinska University hospital and Division of Physical Therapy, Department of NVS and Division of Rheumatology, Department of Medicine, Karolinska Institutet, Stockholm, Sweden

[7]Function Area Occupational Therapy and Physical Therapy, Karolinska University Hospital and Swedish Rheumatism Association, Stockholm, Sweden

Abstract

The etiology of myositis is unknown. Although attempts to identify viruses in myositis skeletal muscle have failed, several studies have identified the presence of a viral signature in myositis patients. Here we postulate that in individuals with susceptible genetic backgrounds, viral infection alters the epigenome to activate the pathological pathways leading to disease onset. To identify epigenetic changes, methylation profiling of Coxsackie B infected human myotubes and muscle biopsies from polymyositis (PM) and dermatomyositis (DM) patients were compared to changes in global transcript expression induced by *in vitro* Coxsackie B infection. Gene and protein expression analysis and live cell imaging were performed to examine the mechanisms. Analysis of methylation and gene expression changes identified that a mitochondria-localized activator of apoptosis – harakiri (HR) – is up-regulated in myositis skeletal muscle cells. Muscle cells with higher HRK expression have reduced mitochondrial potential and poor ability to repair

[*]**Correspondence to**: Kanneboyina Nagaraju, Department of Pharmaceutical Sciences School of Pharmacy and Pharmaceutical Sciences, Binghamton University, PO Box 6000, Binghamton, NY, USA Phone: 607-777-5814. Nagaraju@binghamton.edu, or Jyoti Jaiswal, Center for Genetic Medicine Research, Children's National Health System, 111 Michigan Avenue, NW Washington, DC, USA. Phone: 202-476-6456. jkjaiswal@childrensnational.org.

Raw data of experiments using array-based technology is available at https://www.ncbi.nlm.nih.gov/gds/?term=nagaraju (GSE95735_RAW.tar)

from injury as compared to controls. In cells from myositis patient Toll-like receptor 7 (TLR7) activates and sustains high HRK expression. Forced over expression of HRK in healthy muscle cells is sufficient to compromise their membrane repair ability. Moderate training exercise that is associated with improved muscle and mitochondrial function in PM and DM patients decreased *TLR7* and *HRK* expression identifying these as therapeutic targets. Increased HRK and TLR7 expression causes mitochondrial damage leading to poor myofiber repair, myofiber death and muscle weakness in myositis patients and exercise induced reduction of HRK and TLR7 expression in patients is associated with disease amelioration.

Introduction

Idiopathic inflammatory myopathy (IIM), or myositis, is characterized by chronic symmetrical proximal muscle weakness, muscle fatigue, mononuclear cell infiltration in skeletal muscle tissue, and presence of autoantibodies to ubiquitous cellular antigens. Both adaptive immune and non-immune mechanisms have been proposed to cause muscle fatigue and muscle damage [1]; however, the basis for the initiation and perpetuation of these mechanisms and the downstream pathways through which they cause muscle weakness and damage has remained unresolved.

Although the etiology of myositis is currently unknown, disease onset in a subset of individuals has been associated with environmental agents, suggesting that specific exposure, in the context of certain genetic backgrounds, can initiate disease onset. Common environmental agents implicated in myositis include infectious organisms, such as viruses, parasites, and bacteria, as well as non-infectious agents, such as drugs (e.g., statins) and UV radiation exposure [2–4]. Attempts to identify viruses in the tissues of IIM patients have failed, bringing into question the viral etiology of these diseases and ruling out continual viral infection as a cause of the ongoing muscle inflammation in these patients [5]. Despite the absence of viral genomes, the presence of type I interferon signature gene expression in myositis muscle tissue provides support to the disease being initiated by a viral infection [6–9]. Such a mode of initiation also requires that instead of a continued viral presence, a sequalae of the viral infection through a mechanism such as a change in the epigenome of the infected cells may sustain the disease following its initial onset by the viral or other environmental factor.

Coxsackie B virus is an environmental agent implicated as one of the likely viral triggers for initiating myositis pathogenesis [2]. Coxsackie B is a single-stranded RNA enterovirus that activates the innate immune system via toll-like receptor 7 (TLR7) and causes flu-like symptoms. Evidence of Coxsackie B in myositis include reports of positive serological titers against multiple Coxsackie B viral antigens in PM and DM patients [10, 11]. Further, injection of Coxsackie B into mice with a susceptible genetic background (CHO mice) has been shown to induce features compatible with myositis [32].

Not only has Coxsackie B been linked to myositis, but also mitochondrial abnormalities have been frequently associated with inclusion body myositis, polymyositis and dermatomyositis [12–16]. Further, recent studies looking at the metabolic effects after exercise in myositis muscle suggest a potential role for mitochondria in disease pathology.

Historically, due to the characteristic signs of muscle damage and inflammation, physicians have avoided prescribing exercise to improve mitochondrial function in myositis patients. Recently, by analyzing the transcriptomic and proteomic changes in myositis patients after 12 wk of endurance exercise training, we described that genes related to mitochondrial health and biogenesis were upregulated, which correlated with improved measures of skeletal muscle performance in these patients [17]. Aside from the widely recognized metabolic role of mitochondria in skeletal muscle, we have previously identified a role of mitochondria in facilitating the repair of injured skeletal myofibers [18, 19]. We found that progressive dysfunction of mitochondria in dystrophin deficient muscle contributes to skeletal myofiber damage and ensuing inflammation of the muscle [20].

In this study, we have explored the hypothesis that viral infection-induced epigenetic changes triggered at the time of disease onset alters mitochondrial and cellular function creating a self-sustaining feedback loop responsible for persistent muscle damage in myositis patients.

Methods

Ethics.

This study was approved by the local ethics committee at Karolinska University Hospital and the Institutional Review Board at Children's National Medical Center, Washington, DC, USA.

Muscle biopsies from myositis patients.

Deidentified PM and DM biopsies (n=8) and healthy muscle biopsies (n=4) were obtained from Dr Ingrid Lundberg, Karolinska Institutet for exercise studies as described previously [12, 17, 21]. In brief, muscle biopsies were frozen in liquid nitrogen-cooled isopentane, and stored at −80°C until analysis.

The exercise intervention consisted of 30 min of stationary biking at a power requiring 70% of VO_2 max and did endurance resistance training to exhaustion. The total exercise time per session was 60 min. Patients exercised under supervision for 3 d each week for 12 weeks. Expression profiling data (Illumina, San Diego, CA, USA) from these samples were used for validation of genes identified via muscle biopsy and *in vitro* viral cell culture comparisons.

Cell culture.

Primary human myoblasts from healthy (Lonza) and PM/DM patient myoblasts (Dr Marina Mora, EuroBioBank, Milan, Italy) were grown at 5,000 cells/cm^2 in 0.4% gelatinized flasks with complete Ham's F10 medium. For differentiation, 26,000 cells/cm^2 were plated onto 0.4% gelatinized plates. The following day, growth media was removed and differentiation medium containing 2% horse serum was used for 3 d.

Gene expression profiling.

Total RNA from healthy and Coxsackie-infected human myotubes was extracted using Trizol according to the manufacturer's protocol. After ensuring quality and purity using the

Agilent 2100 Bioanalyzer, global gene expression was assessed using the Illumina HumanHT-12 v4 microarray and analyzed by the GenomeStudio™ Gene Expression Module, which is an integrated platform for data visualization and analysis. The data is available as GSE95735_RAW.tar.

Methylation profiling.

Methylation profiling was performed using the Infinium Human Mehtylation 450K Beadchip kit (Illumina, San Diego, CA, USA). In brief, Genomic DNA was extracted from muscle biopsies and cultured muscle cells using phenol/chloroform and treated with sodium bisulfite following the manufacturer's instructions. Samples were loaded into Beadchips to assess the methylation status across the entire genome. Subset normalization was performed using SWAN (doi: 10.18129/B9.bioc.minfi, 2010) and batch correction was applied using ComBAt. Statistics, visualization, and integration were carried out with both Partek and the UCSC Genome Browser (https://genome.ucsc.edu/, 2010)

Data analysis.

Genes potentially altered by change in the epigenome due to onset of myositis (patient biopsies) or viral infection (Coxsackie infected myotubes) were identified by methylation profiling [22]. Comparison between these groups identified a subset of shared genes. These genes were then compared to the list of genes that had significantly altered mRNA expression after Coxsackie B infection. Doing so provided a list of 39 candidate genes that showed altered expression as a result of epigenetic change in both viral infected muscle cells and patient biopsies. For all analyses, statistical significance was defined as $p<0.05$ with the aim of hypothesis generation.

RT-qPCR.

Aliquots (400 ng) of total RNA isolated from muscle biopsies and cultured muscle cells were reverse transcribed using qScript (Quanta Bio, Beverly, MA) according to the manufacturer's protocol. Then, 10 ng of cDNA were analyzed in triplicate using TaqMan Universal PCR Master Mix II with the following probes: *HRK* (Hs02621354_s1), *TLR7* (Hs01933259_s1), and *HPRT*1 (Hs02800695_m1) (Thermo Fisher Scientific, Waltham, MA, USA) using standard cycling conditions. Data were quantified using the ΔΔCt method with all data normalized to hypoxanthine guanine phosphoribosyltransferase 1 (*HPRT1*).

Western blotting.

Total protein was extracted from frozen muscle tissues were subjected to Western blotting and probed with antibodies against HRK (PRS3771,1:1000; Sigma, St. Louis, MO, USA) or vinculin ([SPM227], ab18058, 1:1000, Abcam, Cambridge, MA, USA) and polyclonal horse anti-mouse HRP antibody or polyclonal goat anti–rabbit HRP antibody (1:5000; Cell Signaling, Danvers, MA, USA). Ratios of the optical density of each specific protein band were normalized to the corresponding loading control (anti-vinculin).

Immunofluorescence.

Frozen healthy muscle tissues were cut at 10 μm and sections fixed in acetone. Sections were stained with anti-HRK (PRS3771,1:100, Sigma), anti-mitochondrial HMS-0300 (HMS-0300, 1:100, Immunovision, Springdale, AK, USA), and anti-laminin 2A 4H8–2 (ALX-804–190-C100, 1:100, Enzo Lifesciences, Farmingdale, NY, USA) and goat anti-rabbit IgG Alexa 488 antibody, mouse anti-human IgG Alexa 647 antibody, and donkey anti-rat IgG Alexa 568 (1:500). Images were acquired using a confocal Olympus FV1000 microscope.

Flow cytometry.

Myoblasts were trypsinized and resuspended in 1 ml of growth media (~200,000 cells/ml). Cells were incubated with TMRE dye (150 nM) for 20 min at 37 °C, washed in PBS with 0.6% BSA, and resuspended in 1 ml of PBS with 0.6% BSA. Samples were processed on a FACSCalibur (BD Biosciences, Sparks, MD, USA) using the FL2 region (574, 573 nm)

Plasma membrane repair assay.

Cells grown on 0.4% gelatinized coverslips were washed once with pre-warmed cell imaging medium (CIM); HBSS (Sigma) with 10 mM HEPES (Thermo Fisher Scientific) pH 7.4 and 2mM Ca^{2+}) at 37 °C and then transferred to CIM containing 1.66 μg/μl of FM1–43 dye (Thermo Fisher Scientific). Cells were injured by irradiating a 1–2 μm^2 area for <10 milliseconds with a pulsed laser (Ablate!, Intelligent Imaging Innovations, Inc., Denver, CO, USA)). Repair kinetics were monitored as described previously [23] using an inverted Olympus IX81 microscope custom equipped with a CSUX1 spinning disc confocal unit (Yokogawa Electric Corp., Sugar Land, TX), pulsed laser Ablate!, and diode laser excitation at 488 nm and 561 nm. FM1–43 dye fluorescence in the cells was measured and the change in intensity (F/F_0) plotted as average ± SEM for each group.

Cell viability measurement.

Myoblasts were plated (5,000 cells/well) in a 96-well plate and supplemented with growth media. The following day, 10 μl of CCK-8 reagent was added to each well and incubated at 37 °C for 4 h. The absorbance of recovered dye at 450 nm was used to estimate the effect of treatments on cell number by comparing to an untreated control.

Results

Identification of DNA methylation and gene expression changes in Coxsackie B6 virus-infected human skeletal muscle cells and myositis patient muscle biopsies.

To identify genes affected by an altered epigenome in myositis, we performed methylation profiling on muscle biopsies from eight patients with DM and PM and compared methylation changes to healthy controls. This analysis identified that the methylation status of 6865 genes was significantly altered in the patient muscles (Supplementary material, Table S1). To determine which of these genes methylation status could have been altered due to a previous viral infection, we independently performed comparative methylation profiling of genomes of primary human myotubes that were (or were not) infected with Coxsackie B6

virus. We infected primary human myotubes with Coxsackie B6 virus (ATCC #VR-155 - prepared by serial passages in skeletal muscle cells) at a standardized dose of 8 MOI (multiplicity of infection) for 120 h. Methylation profiling of genomic DNA identified 1836 total genes that showed altered methylation status (Supplementary material, Table S2). Of these genes, 508 were shared between both patient muscle biopsies and Coxsackie B infected myotubes. To further narrow down the candidate genes, we examined which of these genes were altered in their expression with respect to methylation status. mRNA profiling of the viral-infected human myotubes identified a total of 1595 genes with altered expression of which merely 39 genes had concurrently altered methylation status in myositis patients and virus infected versus uninfected myotubes (supplementary material, Table S3, and Figure 1A). These genes represent the putative list of genes that could potentially initiate viral infection-triggered disease pathogenesis in myositis patients (Table 1, Figure 1A).

We looked closely at genes that may be linked to increased death of myofibers in myositis patients. Of the 3 genes linked to cell death (Table 1) one of the genes identified is a mitochondria-localized protein harakiri (HRK). HRK is known for its ability to facilitate apoptotic cell death by increasing mitochondrial outer membrane permeabilization (MOMP) [24, 25]. Mitochondrial dysfunction has been frequently observed in the myositis patients [12, 26, 27]. Thus, we investigated the role of HRK in myositis patients.

First, to validate our findings from the omics analysis we used western blotting and RT-qPCR as independent assays to examine the expression of *HRK* in response to disease. Using RT-qPCR we found nearly a 10-fold increase in *HRK* transcript levels in myositis patient muscles as compared to healthy controls (Figure 1B). We next examined if increase in *HRK* transcript level results in subsequent increases at the protein level in the patient muscles. Using a random subset of four of the myositis patients as our validation cohort we found that the increase in *HRK* transcript also resulted in a significant 16-fold increase in HRK protein in myositis muscle when compared to healthy muscles (Figure 1C).

Mitochondria-localized HRK is increased in myositis muscle cells and causes cell death.

HRK is known to interact with and inhibit the anti-apoptotic BCL-2 protein, which is associated with the mitochondrial outer membrane [25]. We performed immunofluorescence staining for mitochondria and HRK in healthy human skeletal muscle sections and cultured myoblasts (Figure 2A) to see whether HRK localizes to mitochondria in skeletal muscle as well.

Our findings above showed that *HRK* expression is increased in myositis patient biopsies compared to healthy biopsies and *HRK* expression is also increased in Coxsackie B virus infected as compared to the uninfected cells. Therefore, we next examined whether *HRK* expression was also elevated in myoblasts obtained from patients that already manifest the myositis symptoms to show that increased *HRK* expression in patient biopsies is from muscle cells but not due to immune cell infiltration. Furthermore, we reasoned that if *HRK* expression was driven by decreased methylation in its promoter region, then patient myoblasts may maintain this epigenetic imprint and cause higher levels of *HRK* gene expression as compared to healthy primary myoblasts. We assessed the *HRK* gene

expression in primary myoblasts isolated from two dermatomyositis patients (DM1/DM2) and two polymyositis patients (PM1/PM2) obtained from Dr. Marina Mora through the EuroBioBank (www.eurobiobank.org, accessed 2014). Analysis of *HRK* gene expression by RT-qPCR showed that compared to the healthy control myoblasts, each patient's myoblasts showed a significantly greater level of *HRK* gene expression (Figure 2B).

Given the role of HRK in directly inhibiting the BCL-2 family of anti-apoptotic proteins, we next assessed whether increased HRK expression in patient myoblasts is associated with a change in cell viability [28]. We found *HRK* expression level is indeed inversely correlated with the cell viability, with the patient myoblasts having the greatest *HRK* expression (DM2) showing the least cell viability while the patient with the least increase in *HRK* (DM1) showed greatest cell viability (Figure 2C). Further, cell viability changes correlated more with *HRK* expression level and appeared to be independent of the form of the disease itself - DM versus PM. These data support the link between HRK increase in myositis patients with greater skeletal muscle cells death. We next examined if this link is due to HRK-dependent mitochondrial dysfunction in skeletal muscle.

HRK-induced mitochondrial dysfunction causes poor plasma membrane repair.

To test whether increased HRK expression resulted in mitochondrial depolarization in myositis patient myoblasts we performed flow cytometry to measure the intensity of the dye TMRE, which labels mitochondria based on the potential across the inner mitochondrial membrane [29]. We first confirmed the validity of this approach by treating healthy myoblasts with carbonyl cyanide m-chlorophenyl hydrazine (CCCP), a protonophore that results in mitochondrial membrane depolarization. This resulted in a significant decrease in TMRE (Figure 3A). We next tested whether myositis patient myoblasts had a similar decrease and found that, similar to CCCP treated healthy myoblasts, mitochondrial membrane potential was significantly reduced in myoblasts from patients when compared to healthy controls (Figure 3A).

Thus, we sought to identify a mechanism by which increased *HRK* expression can cause myofiber death and result in muscle pathology in myositis patients. Our previous studies have identified a requirement of mitochondria for the successful repair of plasma membrane following injury to myofibers and myoblasts [18, 19].

To determine if mitochondrial dysfunction caused by increased *HRK* expression in myositis patients also causes poor plasma membrane repair, we subjected healthy and myositis patient myoblasts to a focal laser injury protocol we have previously employed [23]. Using this approach, cells were injured in the presence of a membrane impairment dye (FM 1–43) and dye uptake was monitored following focal plasma membrane injury. Increased dye uptake indicates poor plasma membrane repair due to the delay in the closure of the plasma membrane wound. We first confirmed that mitochondrial depolarization resulted in poor plasma membrane repair by treating healthy myoblasts with CCCP, which caused a significant increase in FM-143 dye entry and the number of cells that failed to repair from focal laser injury (Figure 3B–D). To assess the role of HRK-mediated depolarization on plasma membrane repair we next injured myositis patient myoblasts. Following injury, myositis patient cells allowed significantly greater dye uptake compared to healthy control

myoblasts indicating delayed kinetics of plasma membrane repair (Figure 3E). Additionally, significantly more myositis patient myoblasts failed to successfully repair from plasma membrane injury (Figure 3F). To conclusively establish if it is indeed the HRK expression that is the cause of poor plasma membrane repair in these patient cells, we transiently overexpressed HRK in healthy myoblasts. Upon injury, healthy control myoblasts overexpressing HRK repaired significantly worse than mock-transfected myoblasts indicating that increase in HRK is sufficient to cause poor plasma membrane repair (Figure 3G–I).

Activation of innate immune response induces *HRK* transcription.

A consequence of poor plasma membrane repair is the leakage of intracellular constituents, such as nucleic acids and ATP, into the extracellular space where they can act as damage-associated molecular patterns (DAMPs) to activate an inflammatory response. One such pro-inflammatory pathway of relevance to skeletal muscle pathology in myositis is the innate immune signaling regulated by TLR7, a known receptor for Coxsackie B virus. Mining publicly available Chip-seq data (Qiagen Database, accessed 2016), we found the presence of NF-κB elements in the promoter of *HRK* suggesting that *HRK* expression may be under the control of toll-like receptors such as TLR7 (Figure 4A). Thus, we hypothesized that HRK-induced poor plasma membrane repair may cause an increase in pro-inflammatory TLR7 response. In the myositis patient biopsies, we found *TLR7* expression to be significantly increased compared to healthy control samples (Figure 4B). Due to the presence of infiltrating immune cells that express TLR7 in patient muscle tissue, we next examined if skeletal muscle cells contributed to the increased *TLR7* expression independently of inflammation. RT-qPCR analysis of myositis patient myoblasts showed that similar to patient biopsies, *TLR7* expression was significantly increased in the cultured patient myoblasts (Figure 4C). Thus, *TLR7* expression in myositis patients may lead to increased expression of NF-κB dependent genes including *HRK*.

With a direct NF-κB mediated link between increased co-expression of *TLR7* and *HRK* in myositis patient muscle cells, we hypothesized that a muscle-intrinsic feedback loop may be the basis for sustained increase in expression of these genes. To test this hypothesis, we treated healthy human myoblasts with single stranded RNA (ssRNA) to activate NF-κB and transcription of pro-inflammatory cytokines mediated by its binding to *TLR7* [30]. ssRNA treatment of healthy myoblasts led to significant increase in the expression of both *TLR7* and *HRK* (Figure 4D, E). To independently examine if this increase is mediated by the action of TLR7, and not by some other mode of action of ssRNA, we treated healthy myoblasts with varying doses of a synthetic TLR7 agonist - gardiquimod. Gardiquimod treatment resulted in a dose-dependent increase in both *HRK* and *TLR7* expression (Figure 4F, G) as well as significantly decreased viability of healthy myoblasts (Figure 4H).

Exercise reduces *HRK* and *TLR7* expression in myositis patients.

Previous studies have shown that endurance exercise improves mitochondrial function by increasing expression of components required for oxidative phosphorylation [17]. This was seen at the functional level in myositis patients with exercise resulting in increased aerobic capacity after 12 wk [21].

Myositis patients (6 out of 9) also showed decreased serum CK after the exercise intervention, suggesting that exercise may help patients with muscle damage [21]. This led us to hypothesize that exercise-induced improvement in mitochondrial function may disrupt the feed-forward loop discussed above by preventing increase in *HRK* and *TLR7* levels. To assess this, we obtained paired muscle biopsies from three patients that underwent the moderate intensity exercise intervention. Patients were biopsied before and after the 12 weeks of exercise intervention, which consisted of endurance exercise for one hour, three times per week (Figure 5A). We quantified *HRK* and *TLR7* transcripts in these paired patient muscle biopsies, which showed that both *HRK* and *TLR7* gene expression levels were significantly decreased in myositis patients after the endurance exercise intervention (Figure 5B, C). Thus, endurance exercise improved mitochondrial function by slowing disease progression through a reduction in *HRK* and *TLR7* gene expression. This prevents the establishment of an HRK-TLR7 driven feed-forward loop that underlies pathogenesis of this disease (Figure 5D).

Discussion

The environmental triggers of myositis are likely to be diverse and unrelated to each other (virus, bacteria, drugs, smoking and UV exposure); however, most of the environmental triggers are also known to cause epigenetic modifications in the host cell genome [31]. Here we have shown that the epigenome at the promoter site of the pro-apoptotic mitochondrial gene, harakiri (*HRK*), is altered leading to increased expression of HRK and mitochondrial dysfunction in myositis. We also demonstrate that HRK-induced mitochondrial dysfunction causes poor plasma membrane repair in skeletal muscle cells from myositis patient, potentially leading to leakage of endogenous toll-like receptor (TLR) ligands. We have identified that TLR7 agonist increase *HRK* expression in myositis. Our data explains the self-sustaining nature of muscle damage and progression of muscle weakness in myositis.

Although no known genetic mutations cause myositis, it has been hypothesized that epigenetic alterations may cause the disease phenotype [2, 5, 32–35]. For our experiments, Coxsackie B virus was used as a putative etiological agent for myositis based on the vast amount of previous data implicating this virus in skeletal muscle damage and inflammation [10, 11, 34–39]. The epigenetic modifications associated with viral infections are likely to alter the expression of genes that both initiate and sustain pathological effects in those with susceptible genetic backgrounds (e.g., HLA). A variety of viruses cause tissue damage and human disease. In healthy individuals, once the virus is eliminated by the immune system, affected tissues recover from virus-induced damage and normalcy ensues (Figure 5D). However, our results show that epigenetic changes in the host genome caused by viruses, and not the virus-induced tissue damage per se, can trigger the autoimmune human disease myositis. By using a genome-wide approach, we investigated whether viral infection alters the epigenome. By measuring methylation and gene expression in virus infected myotubes and comparing this to the epigenetic status of genes in muscle biopsies from patients with myositis we determined a set of common candidate genes that may contribute to myositis pathogenesis. One of the candidate genes we identified is *HRK* - a known modulator of mitochondrial apoptosis. *HRK* was induced by viral infection of skeletal muscle cells and myositis patients had a decrease in methylation in the promoter region of *HRK*.

It is thought that failed repair results in a leaky membrane, causing the release of multiple intracellular contents, such as CK, ATP, calcium, and other DAMPs to drive inflammation into the muscle. One DAMP in particular, ssRNA, has been shown to further exacerbate inflammation and disease phenotype in the *mdx* mouse via TLR7 [40]. We found that *HRK* was induced via activation of *TLR7*, which has been previously shown to be activated upon infection with Coxsackie B virus [41]. This suggests that failed repair could activate a self-sustaining loop through TLR7 signaling by further increasing *HRK* expression and consequent mitochondrial dysfunction and muscle damage.

We and others have previously demonstrated that classical apoptotic cell death (caspase-3 mediated) is rare in myositis muscle partly because of upregulation of anti-apoptotic molecules such as Bcl-2, hILP, and FLIP in myositis [42, 43]. However, skeletal muscle death occurs in muscle fibers of myositis patients, despite the overexpression of Bcl-2, hILP, and FLIP molecules, indicating that alternate forms of cell death, such as autophagy and necrosis, may be involved. We have previously shown that both endoplasmic reticulum (ER) stress and autophagy are involved in myositis pathogenesis [44, 45]. Recent studies also indicate that ER stress response connected to autophagic cell death and components of apoptotic pathways may modulate autophagy through cross-talk [46].

Aside from ER defects, mitochondrial changes are common in myositis patients [12–16, 47]. We have previously identified that a novel role of mitochondria is to facilitate repair of injured myofibers, which is compromised in a dose-dependent manner by mitochondrial depolarization [18]. More recently, we identified that mitochondria facilitate sarcolemmal repair by facilitating injury triggered calcium signaling required for repair [19]. ER-mitochondria interactions are crucial for cellular calcium homeostasis, defects in which lead to disease [48]. Therefore, we postulate that the combined ER and mitochondrial deficit in myositis muscle significantly compromises the survival of muscle fibers.

Proposed model.

We present a novel model to explain the relatively poor correlation between inflammation and weakness in myositis. We propose that harakiri (HRK), induces mitochondrial dysfunction leading to poor sarcolemma repair after injury. Defective mitochondria and poor membrane repair potentially lead to release of endogenous TLR ligands (e.g., ssRNA), activation of TLR signaling, and induction of muscle-derived pro-inflammatory cytokines. TLR7 signaling in skeletal muscle cells induces *HRK* expression leading to a self-sustaining loop in the myositis muscle micro-environment (Figure 5D). This model predicts that enhancing mitochondrial biogenesis (via PGC1α, AICAR) and decreasing inflammatory cytokine signaling in skeletal muscle would improve sarcolemma repair and restore muscle strength in these patients [21].

Supplementary Material

Refer to Web version on PubMed Central for supplementary material.

Acknowledgements:

KN is supported by the National Institutes of Health (R21AI128248-02, R56NS097229-01), the Myositis Association and the US Department of Defense (W81XWH-11-1-0809). We kindly thank Dr Marina Mora at IRCCS Besta and the biobank “Cells, tissues and DNA from patients with neuromuscular diseases”, member of the Telethon Network of Genetic Biobanks (project no. GTB12001), funded by Telethon Italy, and of the EuroBioBank network, for providing us with the patient myoblasts.

IL was supported by The Myositis Association, The Swedish Research Council no K2014-52X-14045-14-3, the Swedish Rheumatism Association, King Gustaf V 80 Year Foundation, supported by grants provided by the Stockholm County Council (ALF project)

Grants or other financial supporters of the study: K.N. is supported by the National Institutes of Health (R21AI128248-02, R56NS097229-01), the Myositis Association and the US Department of Defense (W81XWH-11-1-0809). J.K.J acknowledges support by the NIH grants (R21AI128248, R01AR55686).

Financial competing interests: Dr Lundberg has received honoraria from Bristol Myers Squibb and MedImmune and is currently receiving a research grant from Bristol Myers Squibb and from Astra Zeneca. She is a scientific advisor for Bristol Myers Squibb, and aTyr company and Corbus Pharmaceuticals, Inc.

References

1. Coley W, Rayavarapu S, Nagaraju K. Role of non-immune mechanisms of muscle damage in idiopathic inflammatory myopathies. Arthritis Res Ther 2012; 14: 209. [PubMed: 22546362]
2. Tam PE, Weber-Sanders ML, Messner RP. Multiple viral determinants mediate myopathogenicity in coxsackievirus B1-induced chronic inflammatory myopathy. J Virol 2003; 77: 11849–11854. [PubMed: 14557670]
3. Thompson PD, Clarkson P, Karas RH. Statin-associated myopathy. JAMA 2003; 289: 1681–1690. [PubMed: 12672737]
4. Svensson J, Holmqvist M, Lundberg IE, et al. Infections and respiratory tract disease as risk factors for idiopathic inflammatory myopathies: a population-based case–control study. Ann Rheum Dis 2017; 76: 1803–1808. [PubMed: 28855175]
5. Leff RL, Love LA, Miller FW, et al. Viruses in idiopathic inflammatory myopathies: absence of candidate viral genomes in muscle. Lancet 1992; 339: 1192–1195. [PubMed: 1349938]
6. Wong D, Kea B, Pesich R, et al. Interferon and biologic signatures in dermatomyositis skin: specificity and heterogeneity across diseases. PLoS One 2012; 7: e29161. [PubMed: 22235269]
7. Baechler EC, Bauer JW, Slattery CA, et al. An interferon signature in the peripheral blood of dermatomyositis patients is associated with disease activity. Mol Med 2007; 13: 59–68. [PubMed: 17515957]
8. Greenberg SA, Higgs BW, Morehouse C, et al. Relationship between disease activity and type 1 interferon- and other cytokine-inducible gene expression in blood in dermatomyositis and polymyositis. Genes Immun 2012; 13: 207–213. [PubMed: 21881594]
9. Bilgic H, Ytterberg SR, Amin S, et al. Interleukin-6 and type I interferon-regulated genes and chemokines mark disease activity in dermatomyositis. Arthritis Rheum 2009; 60: 3436–3446. [PubMed: 19877033]
10. Bowles N, Sewry C, Dubowitz V, et al. Dermatomyositis, polymyositis, and Coxsackie-B-virus infection. Lancet 1987; 329: 1004–1007.
11. Christensen ML, Pachman LM, Schneiderman R, et al. Prevalence of Coxsackie B virus antibodies in patients with juvenile dermatomyositis. Arthritis Rheumatol 1986; 29: 1365–1370.
12. Oldfors A, Moslemi A, Jonasson L, et al. Mitochondrial abnormalities in inclusion-body myositis. Neurology 2006; 66: S49–S55. [PubMed: 16432145]
13. Basualto-Alarcón C, Bozán M, Bevilacqua J, et al. AB0176 Mitochondrial dysfunction in idiopathic inflammatory myopathy derived myoblasts. Ann Rheum Dis 2017; 76: 1108.
14. Alhatou MI, Sladky JT, Bagasra O, et al. Mitochondrial abnormalities in dermatomyositis: characteristic pattern of neuropathology. J Mol Histol 2004; 35: 615–619. [PubMed: 15614615]

15. Woo M, Chung SJ, Nonaka I. Perifascicular atrophic fibers in childhood dermatomyositis with particular reference to mitochondrial changes. J Neurol Sci 1988; 88: 133–143. [PubMed: 2852214]
16. Chariot P, Ruet E, Authier F-J, et al. Cytochrome c oxidase deficiencies in the muscle of patients with inflammatory myopathies. Acta Neuropathol 1996; 91: 530–536. [PubMed: 8740235]
17. Munters LA, Loell I, Ossipova E, et al. Endurance exercise improves molecular pathways of aerobic metabolism in patients with myositis. Arthritis Rheumatol 2016; 68: 1738–1750. [PubMed: 26867141]
18. Sharma N, Medikayala S, Defour A, et al. Use of quantitative membrane proteomics identifies a novel role of mitochondria in healing injured muscles. J Biol Chem 2012; 287: 30455–30467. [PubMed: 22778268]
19. Horn A, Van der Meulen JH, Defour A, et al. Mitochondrial redox signaling enables repair of injured skeletal muscle cells. Sci Signal 2017; 10: eaaj1978. [PubMed: 28874604]
20. Vila MC, Rayavarapu S, Hogarth MW, et al. Mitochondria mediate cell membrane repair and contribute to Duchenne muscular dystrophy. Cell Death Differ 2017; 24: 330–342. [PubMed: 27834955]
21. Munters LA, Dastmalchi M, Katz A, et al. Improved exercise performance and increased aerobic capacity after endurance training of patients with stable polymyositis and dermatomyositis. Arthritis Res Ther 2013; 15: R83. [PubMed: 23941324]
22. Nagaraju K, Ghimbovschi S, Rayavarapu S, et al. Muscle myeloid type I interferon gene expression may predict therapeutic responses to rituximab in myositis patients. Rheumatology (Oxford) 2016; 55: 1673–1680. [PubMed: 27215813]
23. Defour A, Sreetama S, Jaiswal JK. Imaging cell membrane injury and subcellular processes involved in repair. J Vis Exp 2014.
24. Tait SW, Green DR. Mitochondria and cell death: outer membrane permeabilization and beyond. Nat Rev Mol Cell Biol 2010; 11: 621. [PubMed: 20683470]
25. Harris M, Thompson C. The role of the Bcl-2 family in the regulation of outer mitochondrial membrane permeability. Cell death and differentiation 2000; 7: 1182. [PubMed: 11175255]
26. Alhatou MI, Sladky JT, Bagasra O, et al. Mitochondrial abnormalities in dermatomyositis: characteristic pattern of neuropathology. J Mol Histol 2004; 35: 615–619. [PubMed: 15614615]
27. Chew E, Araoz C, Sun C, et al. Dermatomyositis: ultrastructure of abnormal mitochondria in the skeletal muscle. Ann Clin Lab Sci 1977; 7: 29–34. [PubMed: 836001]
28. Inohara N, Ding L, Chen S, et al. harakiri, a novel regulator of cell death, encodes a protein that activates apoptosis and interacts selectively with survival-promoting proteins Bcl-2 and Bcl-XL. EMBO J 1997; 16: 1686–1694. [PubMed: 9130713]
29. Perry SW, Norman JP, Barbieri J, et al. Mitochondrial membrane potential probes and the proton gradient: a practical usage guide. Biotechniques 2011; 50: 98. [PubMed: 21486251]
30. Diebold SS. Recognition of viral single-stranded RNA by Toll-like receptors. Adv Drug Deliv Rev 2008; 60: 813–823. [PubMed: 18241955]
31. Ho S-M, Johnson A, Tarapore P, et al. Environmental epigenetics and its implication on disease risk and health outcomes. ILAR J 2012; 53: 289–305. [PubMed: 23744968]
32. Xiang Z, Yang Y, Chang C, et al. The epigenetic mechanism for discordance of autoimmunity in monozygotic twins. J Autoimmun 2017; 83: 43–50.. [PubMed: 28412046]
33. Albayda J, Christopher-Stine L. Identifying statin-associated autoimmune necrotizing myopathy. Cleve Clin J Med 2014; 81: 736–741. [PubMed: 25452351]
34. Tam P, Schmidt A, Ytterberg S, et al. Duration of virus persistence and its relationship to inflammation in the chronic phase of coxsackievirus B1-induced murine polymyositis. J Lab Clin Med 1994; 123: 346–356. [PubMed: 8133145]
35. Tam P, Schmidt A, Ytterberg S, et al. Viral persistence during the developmental phase of Coxsackievirus B1-induced murine polymyositis. J Virol 1991; 65: 6654–6660. [PubMed: 1942249]
36. Archard LC, Richardson PJ, Olsen E, et al. The role of Coxsackie B viruses in the pathogenesis of myocarditis, dilated cardiomyopathy and inflammatory muscle disease. Biochem Soc Symp 1987; 53: 51–62. [PubMed: 2847741]

37. Ytterberg S Coxsackievirus B 1 induced murine polymyositis: acute infection with active virus is required for myositis. J Rheumatol 1987; 14: 12–18. [PubMed: 3033235]

38. Ytterberg S, Mahowald M, Messner R. Coxsackievirus B 1-induced polymyositis. Lack of disease expression in nu/nu mice. J Clin Invest 1987; 80: 499–506. [PubMed: 3038960]

39. Ytterberg S, Mahowald M, Messner R. T cells are required for coxsackievirus B1 induced murine polymyositis. J Rheumatol 1988; 15: 475–478. [PubMed: 2837572]

40. Henriques-Pons A, Yu Q, Rayavarapu S, et al. Role of Toll-like receptors in the pathogenesis of dystrophin-deficient skeletal and heart muscle. Hum Mol Genet 2014; 23: 2604–2617. [PubMed: 24368419]

41. Triantafilou K, Orthopoulos G, Vakakis E, et al. Human cardiac inflammatory responses triggered by Coxsackie B viruses are mainly Toll-like receptor (TLR) 8-dependent. Cell Microbiol 2005; 7: 1117–1126. [PubMed: 16008579]

42. Li M, Dalakas MC. Expression of human IAP-like protein in skeletal muscle: a possible explanation for the rare incidence of muscle fiber apoptosis in T-cell mediated inflammatory myopathies. J Neuroimmunol 2000; 106: 1–5. [PubMed: 10814776]

43. Nagaraju K, Casciola-Rosen L, Rosen A, et al. The inhibition of apoptosis in myositis and in normal muscle cells. J Immunol 2000; 164: 5459–5465. [PubMed: 10799913]

44. Nagaraju K, Casciola-Rosen L, Lundberg I, et al. Activation of the endoplasmic reticulum stress response in autoimmune myositis: potential role in muscle fiber damage and dysfunction. Arthritis Rheum 2005; 52: 1824–1835. [PubMed: 15934115]

45. Alger HM, Raben N, Pistilli E, et al. The role of TRAIL in mediating autophagy in myositis skeletal muscle: a potential nonimmune mechanism of muscle damage. Arthritis Rheum 2011; 63: 3448–3457. [PubMed: 21769834]

46. Pattingre S, Tassa A, Qu X, et al. Bcl-2 antiapoptotic proteins inhibit Beclin 1-dependent autophagy. Cell 2005; 122: 927–939. [PubMed: 16179260]

47. Rygiel KA, Miller J, Grady JP, et al. Mitochondrial and inflammatory changes in sporadic inclusion body myositis. Neuropathol Appl Neurobiol 2015; 41: 288–303. [PubMed: 24750247]

48. Rowland AA, Voeltz GK. Endoplasmic reticulum–mitochondria contacts: function of the junction. Nat Rev Mol Cell Biol 2012; 13: 607. [PubMed: 22992592]

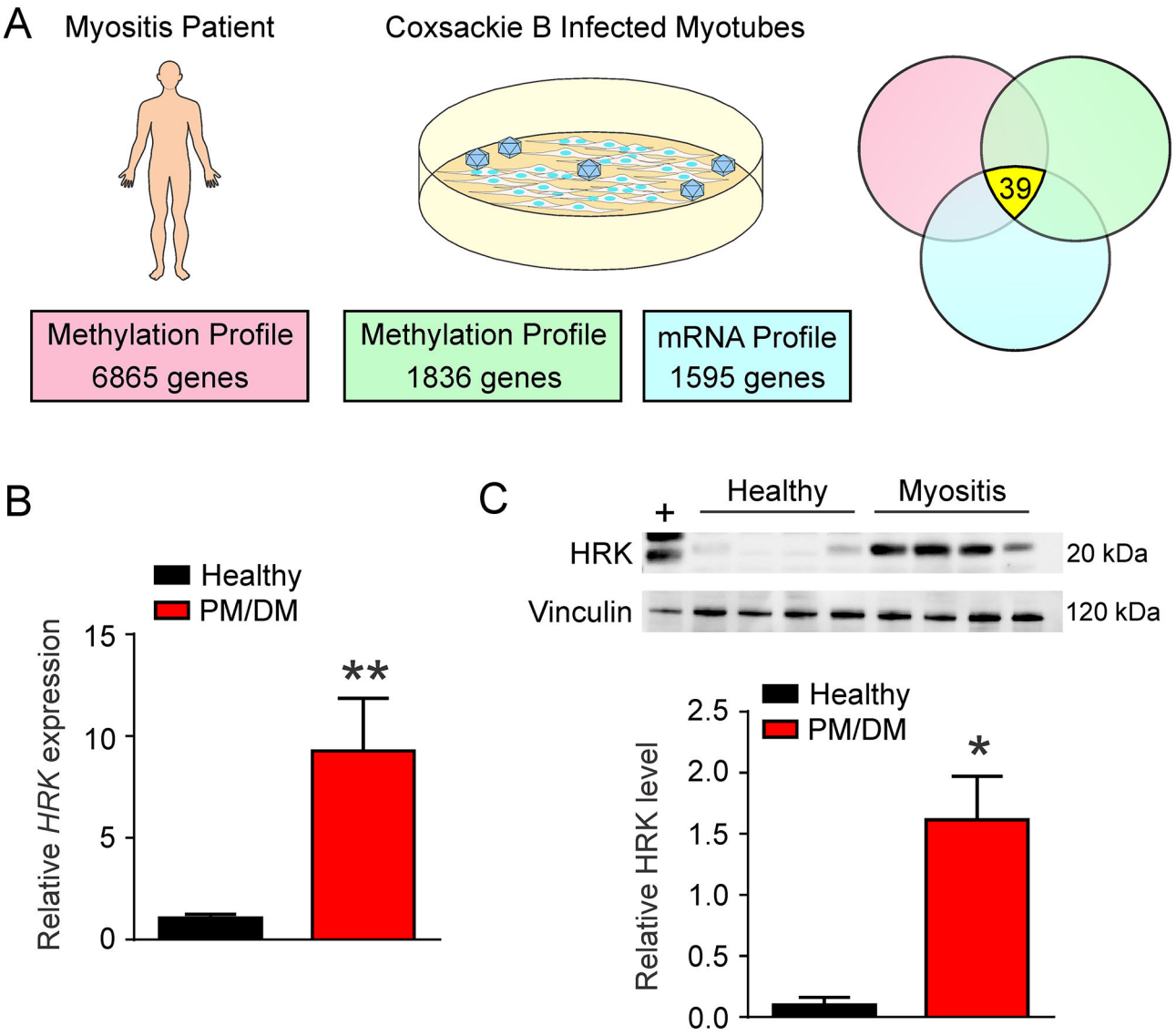

Figure 1. HRK levels are increased in myositis patient skeletal muscle.

(A) Depiction of bioinformatics analysis to identify candidate genes increased in myositis due to virus-induced epigenetic change. Changes in methylation from myositis patient biopsies and Coxsackie B infected human myotubes were compared to gene expression changes in virus-infected myotubes. This identified a set of 39 candidate genes potentially implicated in myositis pathogenesis. (B) Quantification of *HRK* transcripts by RT-qPCR in healthy and myositis patient biopsies (n=4 healthy and 8 myositis patient samples). *HRK* mRNA expression is relative to hypoxanthine guanine phosphoribosyltransferase (*HPRT1*). (C) Western blot showing HRK protein level in healthy and myositis patient biopsies. BL10 pancreas lysates were used as positive control (indicated by '+'). Plot shows average level of HRK relative to the loading control vinculin (n=4 samples each). * $p<0.05$ and ** $p<0.01$ by independent *t*-test.

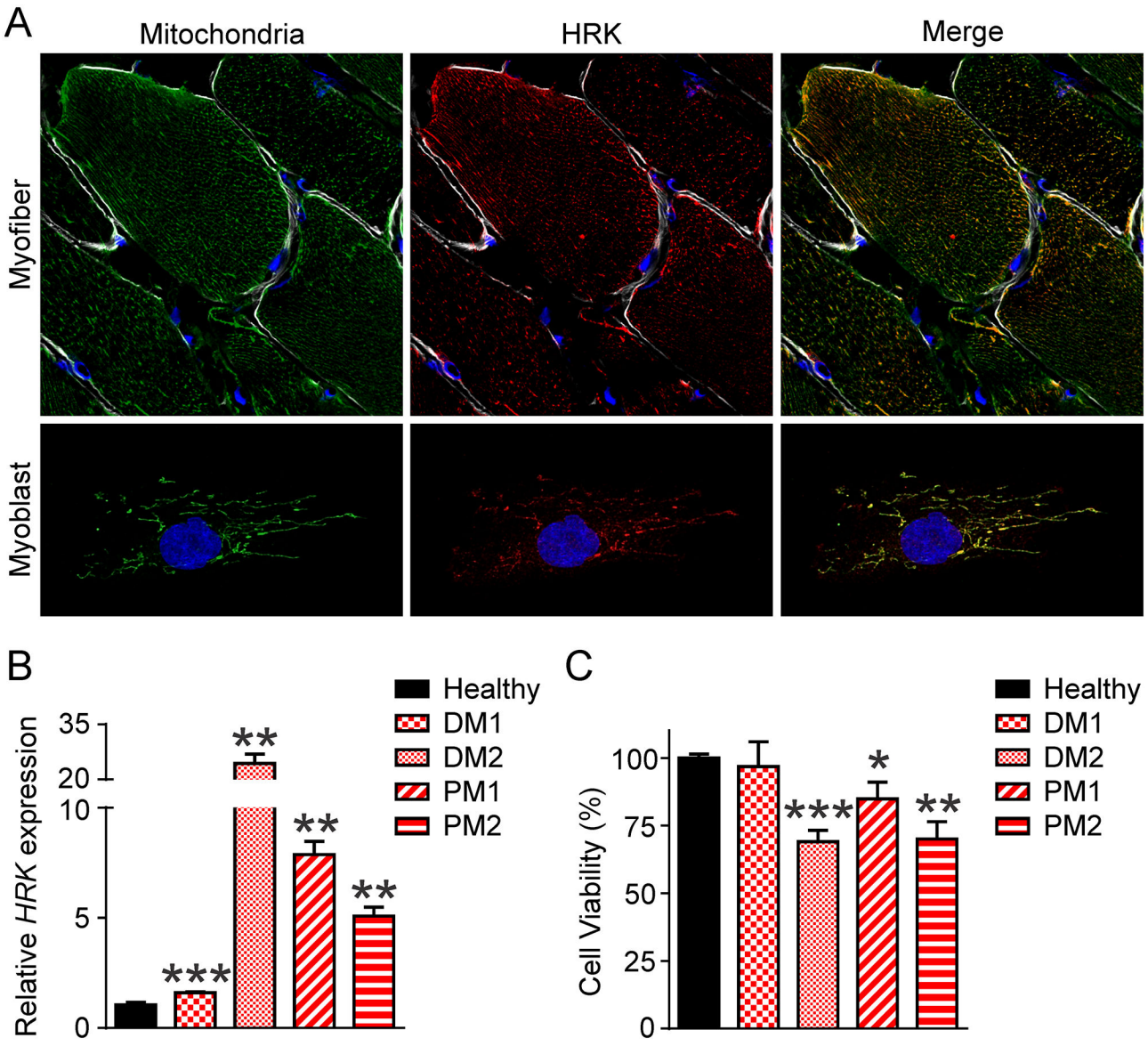

Figure 2. Mitochondria-localized HRK causes cell death in myositis patient myoblasts.

(A) Immunofluorescence images showing localization of HRK in healthy skeletal muscle myofibers and a isolated primary myoblast (Green: HMS-0300- mitochondria). DAPI (blue) indicates location of nuclei. In myofibers, laminin (white) marks the extracellular matrix between individual myofibers. (B) Quantification of *HRK* transcripts by RT-qPCR in myoblasts from healthy individuals and myositis patients (n≥4 replicates each). *HRK* expression is relative to *HPRT1*. (C) Plot showing viability of healthy and myositis patient myoblasts (n≥3 replicates each). * $p<0.05$, ** $p<0.01$, and *** $p<0.001$ by independent *t*-test.

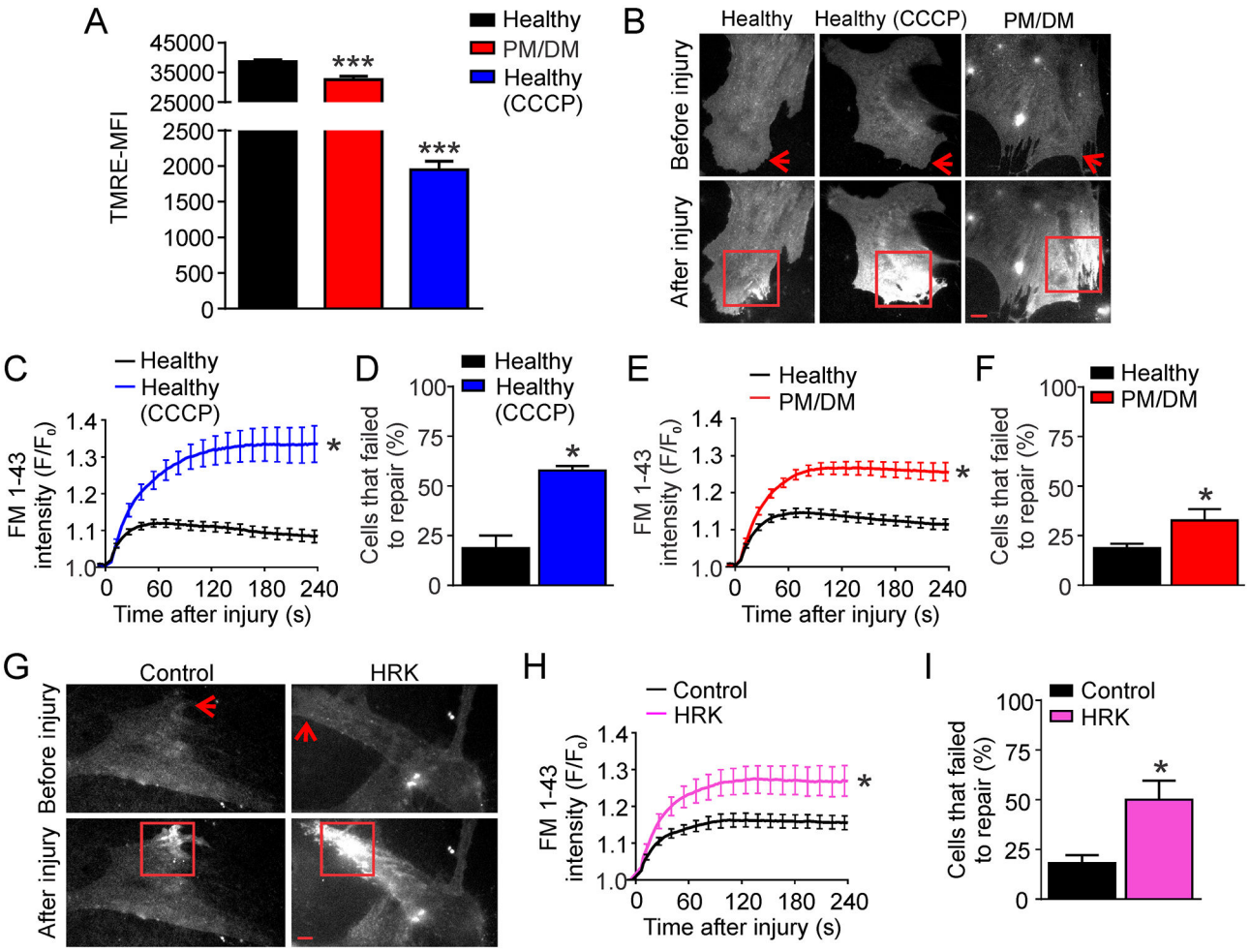

Figure 3. HRK-induced mitochondrial dysfunction causes poor plasma membrane repair.

(A) Plot showing tetramethylrhodamine, ethyl ester (TMRE) fluorescence intensity in healthy and myositis patient myoblasts. As a positive control, healthy myoblasts were treated with 5 μM CCCP to induce mitochondrial depolarization (n=3 replicates each). (B) Images showing FM 1–43 dye entry after focal laser injury in healthy untreated human myoblasts, 5 μM CCCP treated myoblasts, and myositis patient (PM/DM) myoblasts. (C) Quantification of FM 1–43 dye increase in untreated and 5 μM CCCP treated myoblasts (n≥20 myoblasts each). (D) Plot showing number of untreated and 5 μM CCCP treated myoblasts that failed to repair from laser injury (n=2 independent replicates). (E) Quantification of FM 1–43 dye increase in healthy and myositis patient myoblasts (n≥39 myoblasts each). (F) Plot showing number of healthy and myositis patient myoblasts that failed to repair from laser injury (n≥5 independent replicates). (G) Images showing FM 1–43 dye entry after focal laser injury of healthy human myoblasts transfected with fluorescent reporter plasmid - mCherry only (Control) or co-transfected with HRK and mCherry plasmids (HRK) for HRK overexpression. (H) Quantification of increase in FM 1–43 dye fluorescence following injury of transfected (marked by mCherry expression) Control and HRK myoblasts (n≥23 myoblasts each). (I) Plot showing number of Control and HRK

overexpressing cells that failed to repair from laser injury (n=3 independent replicates). * $p<0.05$ and *** $p<0.001$ by independent *t*-test. Scale bar = 10 μm.

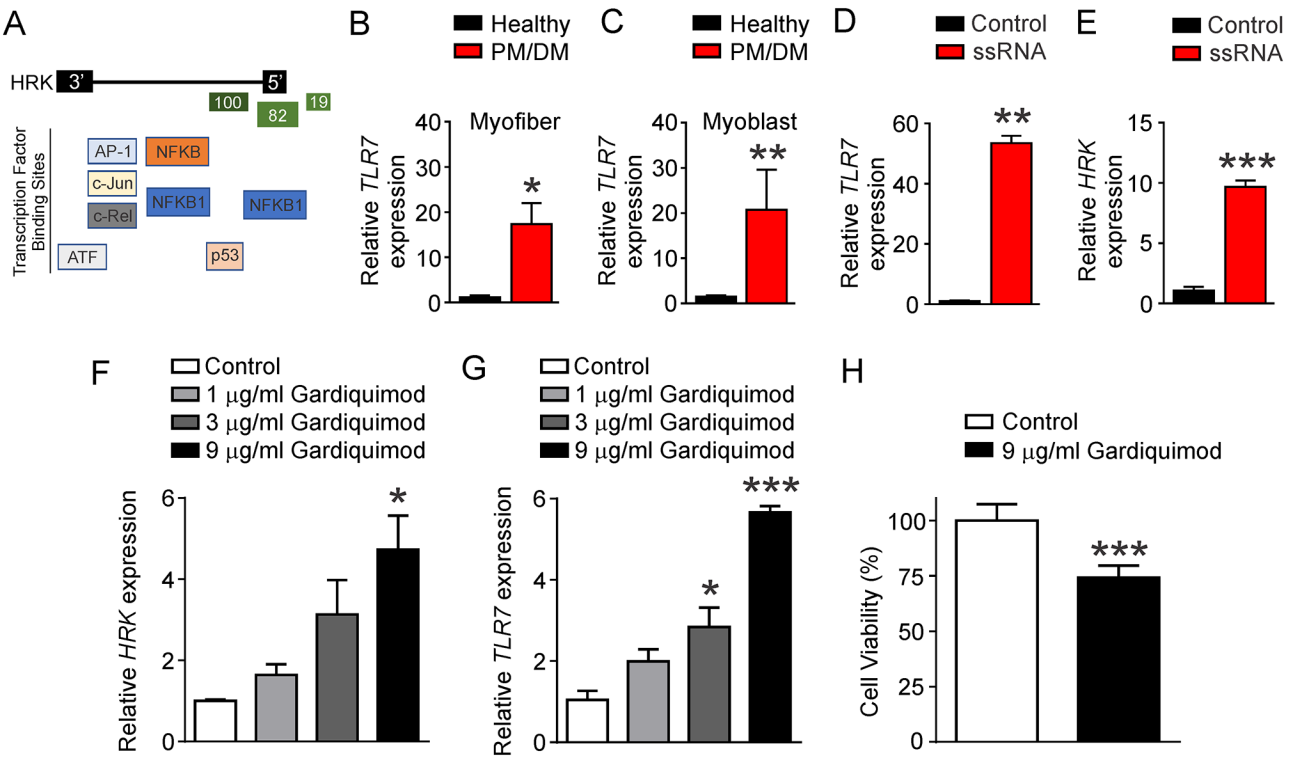

Figure 4, TLR7 regulates increased *HRK* expression.

(A) Schematic showing transcription factor binding sites across the *HRK* gene derived from publicly available ChIP-seq data. (B,C) Quantification of *TLR7* transcripts by RT-qPCR in (B) healthy and myositis patient biopsies (n=4 healthy and 8 myositis patient samples) and (C) healthy and myositis patient myoblasts (n=3 replicates each). (D,E) Quantification of (D) *TLR7* and (E) *HRK* transcripts in myoblasts treated with 3 μg/ml single strand RNA (ssRNA) (n=3 replicates each). (F,G) Quantification of (F) *HRK* and (G) *TLR7* transcripts in myoblasts treated with the indicated concentration of gardiquimod (n = 3 replicates each). (H) Plot showing viability of untreated and gardiquimod treated myoblasts (n≥17 replicates each). In all cases, the expression of the indicated transcript is relative to *HPRT1*. * p<0.05, ** p<0.01, and *** p<0.001 by independent *t*-test.

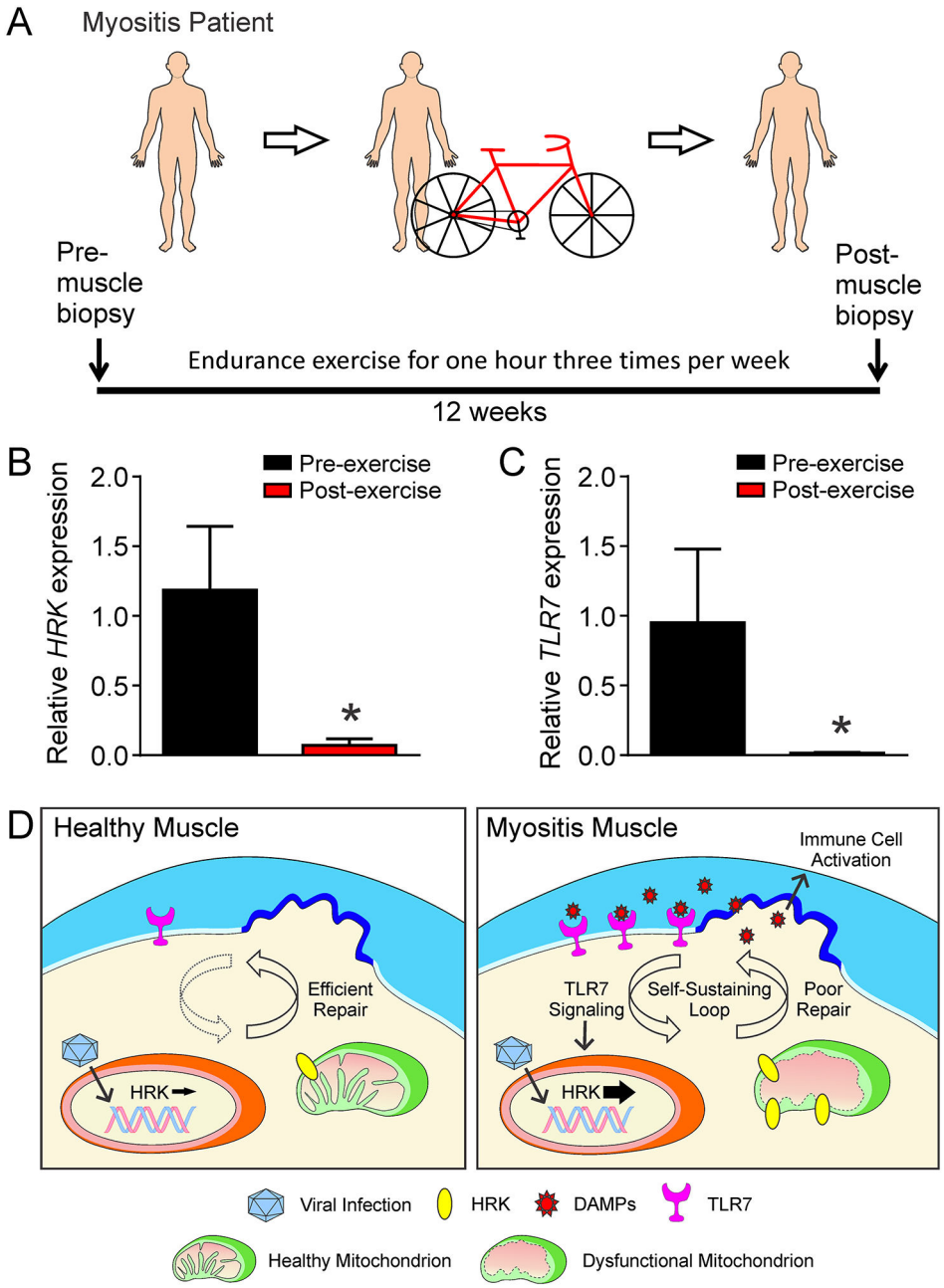

Figure 5. Moderate endurance exercise reduced *HRK* and *TLR7* expression in myositis patients.

(A) Visual representation of 12 wk endurance exercise intervention in which myositis patients underwent one hour of exercise three times per week. (B,C) Quantification of (B) *HRK* and (C) *TLR7* transcripts in myositis patient biopsies before and after a 12-wk endurance exercise intervention (n=3 replicates each). Transcript expression is relative to *HPRT1*. * $p<0.05$ by independent *t*-test. (D) Model for HRK-induced skeletal muscle pathology in myositis.

In healthy muscle, functional mitochondria mediate the efficient repair of injury to damaged sarcolemma (indicated by dark blue shading). In individuals with susceptible genetic backgrounds, viral infection may induce changes in gene expression including a larger

increase in the expression of mitochondrial apoptosis regulatory protein HRK, which causes mitochondrial depolarization compromising efficient myofiber repair. Poor repair of damaged myofibers causes leakage of damage-associated molecular patterns (DAMPs) such as single stranded RNA, which activate TLR7-mediated pro-inflammatory signaling as well as increased *TLR7* expression. This causes increased NF-κB signaling, inducing further increase in HRK expression. This sequence sets in motion a feed-forward loop that exacerbates mitochondrial and myofiber damage, contributing to progressive worsening of the muscle pathology in myositis.

Table 1.

Candidate genes involved in the viral-induced initiation of myositis (**Fold-change relative to control sample**)

Gene Symbol	*In vivo* Methylation	*In vitro* Methylation	*In vitro* mRNA
Cell Death Associated			
TMEFF2	−1.35	12.34	−1.25
MT1X	−1.49	−4.82	1.50
HRK	1.93	4.23	2.28
Biosynthesis and Metabolism			
PFKFB3	−1.62	11.93	−1.39
QPRT	1.31	3.53	1.31
HS3ST3A1	1.30	5.17	1.44
GMDS	−1.42	−2.70	−1.27
XXYLT1	1.44	3.56	−1.43
Signaling, Redox Reactions, and Transcription			
NXN	2.14	76.78	−1.41
EPHA4	1.83	4.57	−1.31
CLSTN2	−1.92	24.05	−1.28
BMPER	1.60	3.74	−1.28
PIEZO2	−1.60	2.70	−1.28
NOTCH3	−1.39	19.23	1.27
NFIX	2.35	5.51	1.29
HOXA9	1.25	2.07	1.33
CYGB	−1.61	8.16	1.42
PLCD1	−1.27	7.48	1.44
CNIH3	1.37	2.31	1.45
LRRFIP1	1.40	41.69	1.49
SGIP1	1.25	2.31	1.54
RSPO3	−3.87	3.38	1.55
NRROS	1.64	18.56	1.69
CAMK2N1	−1.36	11.97	1.98
PRAGMIN	−1.80	2.34	−1.58
Structural - ECM, Cytoskeletal, Cell-Cell Contacts			
COL1A1	−1.56	2.81	−2.13
SERPINH1	−1.51	2.50	−1.54
PXDN	−8.12	3.61	−1.50
CDH11	−2.35	5.42	−1.36
DPYSL4	−1.39	15.15	−1.26
GJB2	1.52	5.47	1.25
PPL	−1.38	5.85	1.26
LRCH2	−1.50	11.40	1.31

Gene Symbol	*In vivo* Methylation	*In vitro* Methylation	*In vitro* mRNA
MXRA8	−1.27	3.83	1.32
FRMD4A	1.46	2.71	1.42
MTSS1	−1.55	4.45	1.64
ODZ4	1.58	2.43	−1.58
KRT19	−1.56	8.63	1.98
SEPT5	−1.34	6.63	−1.69